Simulation of temporal characteristics of ion-velocity susceptibility to single event upset effect*

Geng Chao(耿 超)[a)b)†], Xi Kai(习 凯)[a)b)], Liu Tian-Qi(刘天奇)[a)b)], Gu Song(古 松)[a)b)], and Liu Jie(刘 杰)[a)‡]

[a)] *Institute of Modern Physiscs, Chinese Academy of Sciences, Lanzhou* 730000, *China*
[b)] *University of Chinese Academy of Sciences, Beijing* 100190, *China*

(Received 11 October 2013; revised manuscript received 25 January 2014; published online 10 June 2014)

Using a Monte Carlo simulation tool of the multi-functional package for SEEs Analysis (MUFPSA), we study the temporal characteristics of ion-velocity susceptibility to the single event upset (SEU) effect, including the deposited energy, traversed time within the device, and profile of the current pulse. The results show that the averaged dposited energy decreases with the increase of the ion-velocity, and incident ions of ^{209}Bi have a wider distribution of energy deposition than ^{132}Xe at the same ion-velocity. Additionally, the traversed time presents an obvious decreasing trend with the increase of ion-velocity. Concurrently, ion-velocity certainly has an influence on the current pulse and then it presents a particular regularity. The detailed discussion is conducted to estimate the relevant linear energy transfer (LET) of incident ions and the SEU cross section of the testing device from experiment and simulation and to critically consider the metric of LET.

Keywords: ion-velocity, single event upset, deposited energy, traversed time

PACS: 61.82.Fk, 95.75.–z, 24.10.Lx **DOI:** 10.1088/1674-1056/23/8/086104

1. Introduction

Ion species and energy play an important role in inducing the radiation effects in micro-electronics and aerospace devices. Since single event upset (SEU) was found to be dependent on ion species and energy, major concerns in the ionic characteristic have been recently explored. For instance, Reed *et al.*[1] found through experiment and simulation that the same linear energy transfer (LET) but different ion species and energy resulted in different SEU probabilities. Dodd *et al.*[2,3] explored and discussed the lack of correlation of the SEU cross section with the metric of LET. These studies paid little attention to the ion-velocity on the SEU occurrence. Meanwhile, ion-velocity was preliminarily studied in the field of damage effects by using the swift heavy ions.[4–6] Afterwards, Gaiduk *et al.*[7] observed the ion-velocity effect in the semiconductor materials due to the high-density electron excitation.[7] Additionally, it was found that the ion-velocity effect can be used as the complementary evidence to explain the difference caused by different ion species and energies with the same LET.[8] Thus, the study of the potential damage from the property of ion-velocity in the semiconductor device becomes interesting and meaningful.

The purpose of this work is to investigate the temporal characteristics through the effect of ion-velocity on the SEU occurrence. The multi-functional package for SEEs analysis (MUFPSA) was performed to simulate the SEU probability, the distribution of deposited energy, the traversed time within the device, and the relevant current pulse. Additionally, the SEU cross section is also evaluated through the experiment in the Heavy Ion Research Facility in Lanzhou and the HI-13 Tandem Accelerator. The experimental results support our simulation results.

2. Description of Monte Carlo simulation tool

In this work, Geant4 version 9.3 is used to establish the simulation approach, named MUFPSA. To examine its capability for modeling the SEU characteristics, multiple bit upset (MBU) and SEU susceptibility to the SRAM exposure in the radiation environment have been previously studied. A charge diffusion–collection model and a microscopic model of the ionic characteristc effect are proposed and discussed in this approach.

As a result of the complicated physical process between the ion and materials and according to the previous description of the principle in MUFPSA,[8,9] we use a boson, lepton, hadron, neutron, ion, and decay to accurately describe the ion–device interaction. For the observation of temporal information, the general particle source in Geant4 has been implemented for setting the initiation and then the corresponding energy and time are tracked and recorded. For instance, to characterize the time profile, the equation is given by,

$$t = \sum_{i=0}^{n} [t_i + (t_{i+1} - t_i) \times F_{\mathrm{r}}], \tag{1}$$

where t_i is the time for one initial step, t_{i+1} is the time of next step, and F_{r} is the uniformly distributed random numbers at $[0, 1]$.

*Project supported by the National Natural Science Foundation of China (Grant Nos. 11179003, 10975164, 10805062, and 11005134).
†Corresponding author. E-mail: gengchao@impcas.ac.cn
‡Corresponding author. E-mail: j.liu@impcas.ac.cn
© 2014 Chinese Physical Society and IOP Publishing Ltd

Moreover, the difference in the dispersion of the deposited energy for various ions is used to directly calibrate and improve the accuracy of MUFPSA. The dispersion of deposited energy induced by ^{132}Xe and ^{209}Bi within the sensitive volume (SV) is shown in Fig. 1. The actual deposited energy is measured directly from the incident ion with the specific energy striking on the center of 180-nm Si volume (see the inset). It is illustrated that incident ions of ^{132}Xe with 739 MeV have a wider energy distribution than ^{209}Bi with 385 MeV. Thus, the deviation resulting from the dispersion of deposited energy in terms of different ion species and energy must be absolutely taken into account for describing and analyzing the SEU characteristics.

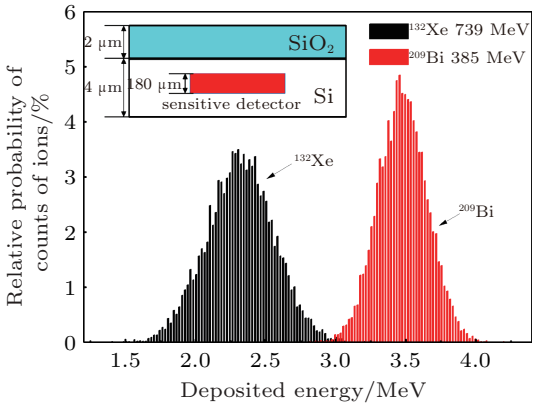


Fig. 1. (color online) Example of the dispersion of deposited energy for ^{132}Xe and ^{209}Bi. The simulation is performed under the condition of striking on the 180-nm Si layer at the center of 4-μm Si volume after the 2-μm SiO_2 layer by the normal incidence (inset).

3. Ion-velocity characterization

The ion-velocity is an intrinsic parameter involved with ion species and energy.[4,5,10] In this work, ion-velocity has been calculated within the framework of relativistic theory using the LISE++ and Mathematica, and in the calculation, the initial energy of the incident ions is used. The ion-velocities of ^{132}Xe and ^{209}Bi are calculated and the results are plotted in Fig. 2, each as a function of ion energy. According to the curves in Fig. 2, the ion-velocity increases nonlinearly with the increment of ion energy. It is noted that the energy discrepancy at the same ion-velocity becomes larger with the increase of ion-velocity. It may be attributed to the fact that the heavier ions with a higher energy have the same ion-velocity as the lighter ions with the lower energy. Consequently, the investigation on the effect of the ionic characteristics on the SEU occurrence is necessary to consider the ion-velocity as a significant representational factor.

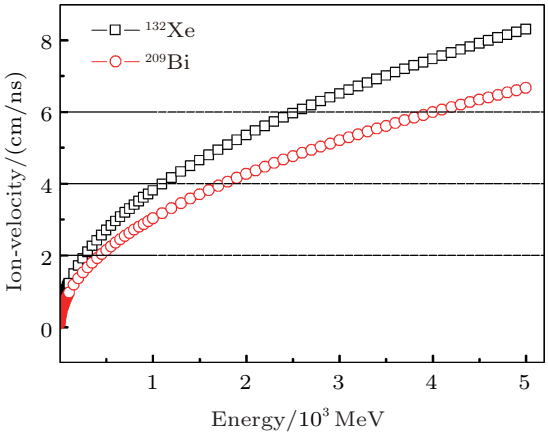


Fig. 2. (color online) Ion-velocities versus the incident ion energy for ^{209}Bi and ^{132}Xe.

4. Results

According to Refs. [11]–[13], the hypothetical device is comprised of an over-layer and substrate. The SVs are properly located at the center of the substrate. The surface area and thickness of silicon film are 2.5 μm×2.0 μm and 0.18 μm, respectively. The way of incidence is defined as randomly striking on the surface of the hypothetical device. The MUFPSA simulation is conducted for 10^4 incident ions to induce the SEU occurrence. The LET of the engineering metric is obtained based on the illustration of Fig. 2, irrespective of the error from the stopping and range of ions in matter (SRIM) professional version calculation. The single errors of ^{132}Xe and ^{209}Bi extracted from the MUFPSA simulation are reported in Table 1. It is shown that the single error basically keeps constant even in the case of the different LETs for different ion species. Thus, no obvious difference in erorr is found for different ion velocities.

Table 1. LET values and SEU errors from ^{132}Xe and ^{209}Bi.

Ion-velocity	^{132}Xe		^{209}Bi	
/(cm/ns)	LET/(MeV·cm^2/mg)	N_{error}	LET/(MeV·cm^2/mg)	N_{error}
2	66.4	2569	93.1	2531
4	61.8	2448	93.4	2565
6	44.9	2351	76.6	2494

The unchanged SEU occurrence is probably explained by the fact that the incident ions with these LET values already have the ability to induce the saturated SEU cross section, which will be further analyzed in Section 5. Because there is no obvious difference in N_{error}, it is promptly demonstrated that the temporal information about the interaction between incident ions and the device, including the distribution of deposited energy, traversed time within the device, and the profile of the current pulse, are of particular importance in assessing the SEU characteristics. Consequently, the above-mentioned temporal information is obtained to expose the micro-differences resulting from the ion-velocity effect.

The results of calculated deposited energy in the hypothetical device on irradiation with the different ion energies are shown in Fig. 3. The relative probability of counts of ions (the vertical axis) is only indicative, since it depends on the histogram representations such as the number of bins setting.

Although the above results of SEU cross sections show no significant difference, the distributions of deposited energy on the same device present a marked difference, even for the incident ions with the same velocity or almost equal value of LET.

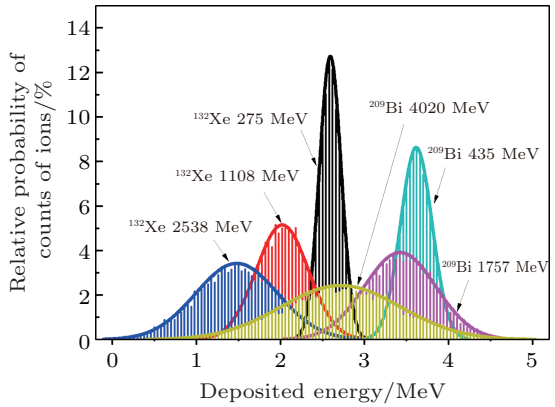


Fig. 3. (color online) Curves of relative probability of count of ions versus measured deposited energy for all the ion energies with ^{132}Xe and ^{209}Bi.

In order to directly compare the results for the measured deposited energy, the full width at half maximum (FWHM) value and absolute difference with respect to the average energy are provided in Table 2. The ratio (R) of the difference between FWHM values of ^{209}Bi and ^{132}Xe to the FWHM value of ^{132}Xe is given as

$$R = \frac{\mathrm{FWHM}_{^{209}\mathrm{Bi}} - \mathrm{FWHM}_{^{132}\mathrm{Xe}}}{\mathrm{FWHM}_{^{132}\mathrm{Xe}}} \times 100\%. \quad (2)$$

As indicated in Table 2, the average deposited energy decreases with the increase of the ion-velocity. This trend results from the integrated effect of the corresponding LET value and the geometrical dimension of the SV. Generally, the higher LET can lead to a higher deposited energy, on condition that the dimensions of volumes are large enough. However, it is probable that the lower LET incident ions induce higher deposited energy within the finite SVs due to the lower ion-velocity and higher initial energy density. For instance, the average deposited energies induced by incident ions ^{209}Bi with the LET of 93.1 MeV·cm^2/mg and 93.4 MeV·cm^2/mg (shown in Table 1) are 3.62 MeV and 3.43 MeV, respectively. On the other hand, the FWHM here is an expression for the extent of the dispersion in the deposited energy. As can be seen from Table 2, considering only one ion species, the FWHM value seems to increase with the augment of ion-velocity. This may be the reason for the fact that the energy loss is reduced by the higher ion-velocity with short traversed time. Additionally, it is inferred that under the condition of the same ion-velocity, the distribution of deposited energies induced by ^{209}Bi is more discrete than by ^{132}Xe. Similarly, the parameter R in Table 2 confirms that the heavier the ion, the larger the distribution of deposited energy is. In our case, the values of R for the ^{132}Xe and ^{209}Bi both can reach a maximum value of 43.6% even with the same ion-velocity. This is also supported by the experimental data.[14] In consequence, ion-velocity dominates the average deposited energy, FWHM, as well as the ratio of FWHM values.

Figure 4 shows the plots of the time of the incident ions transportation within the device and the corresponding deposited energy versus ion-velocity. Overall, a decrease in traversed time is inevitable since ion-velocity plays a crucial role in determining the time in the case of limited distance, and this has already been used for explaining the general trends of variation in average deposited energy and FWHM. In addition, as explained above (see Table 2), the deposited energy is susceptible mainly to the LET value of the incident ion and the volume for collection. Here the regularity of the temporal deposited energy within the SV is recognized as a consequence from the dominant effect of the LET and the strike probability of the Monte Carlo simulation.

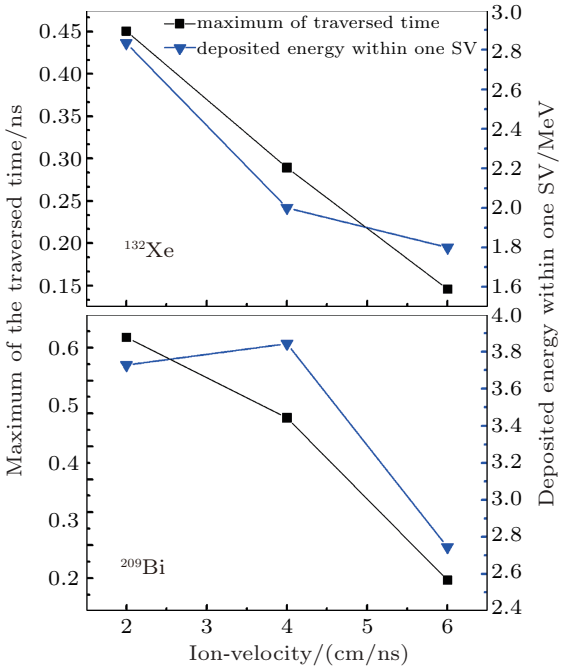


Fig. 4. (color online) Plots of maximum of traversed time and the corresponding deposited energy within the SV versus ion-velocity.

Table 2. The values of average deposited energy E_{ave}, the FWHM, and R obtained through the Gaussian function fitting on Fig. 3.

Ion-velocity/(cm/ns)	^{132}Xe			^{209}Bi			R/%
	E_{ave}/MeV	FWHM/MeV	(FWHM/E_{ave})/%	E_{ave}/MeV	FWHM/MeV	(FWHM/E_{ave})/%	
2	2.59	0.31	11.97	3.62	0.44	12.15	41.9
4	2.03	0.74	36.45	3.43	0.99	28.86	33.8
6	1.48	1.17	79.05	2.72	1.68	61.76	43.6

Additionally, according to Ref. [15], the theoretical method of calculating the amount of charge collection, transporting time of the incident ion, and ion track established time, is a good approach to evaluating the current pulse. The transient currents and the integrated charge collection induced by ^{132}Xe and ^{209}Bi are obtained each as a function of time in Fig. 5. For both ^{132}Xe and ^{209}Bi, the smaller the ion-velocity of incident ions, the larger the width variation is. Also, the transient current induced by heavy ions falls after the peak of the current, the regularity shows that the current at ion-velocity 2 (cm/ns)> that at ion-velocity 4 (cm/ns)> that at ion-velocity 6 (cm/ns). This phenomenon may result from the higher ion-velocity generated higher propagation of initial electron–hole pairs, and then lead to there being less width variation. Moreover, the saturation of collected charge is also consistent with the result of Table 2, showing the relationship as follows: the E_{ave} at ion-velocity 2 (cm/ns)> that at ion-velocity 4 (cm/ns)> that at ion-velocity 6 (cm/ns). The above result is attributed probably to the higher ion-velocity-induced lower concentration of charge initialization, hence the collected charge quantity in limited dimensions of volumes is less. Consequently, from the evaluations of transient current and the relevant collected charge quantity, it is concluded that the ion-velocity does indeed affect the width variation of pulse shape and collected charge quantity due to the ion track profile.

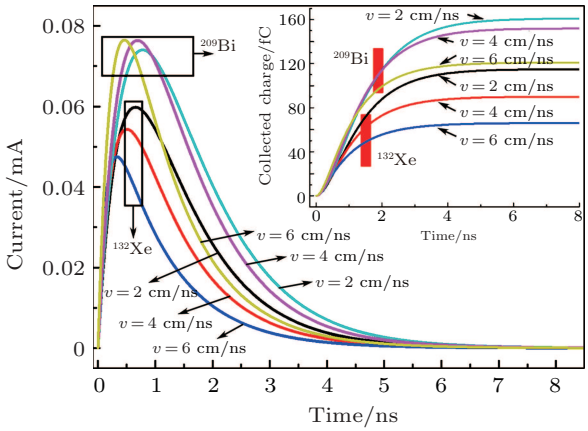


Fig. 5. (color online) Variations of transient current and relevant collected charge quantity with time for several different velocities of the incident ions of ^{132}Xe and ^{209}Bi.

5. Discussion

It is studied in this work that the influence of the ion-velocity on the SEU occurrences may not be reflected directly in the SEU cross section but mainly in the different temporal characteristics, in terms of the distribution of deposited energy, the traversed time on the device, and the profile of the transient current. This approach to the observation of the effect of ion-velocity is also applicable for other devices in the study of ionic characteristics. However, the investigation of the SEU susceptibility to the intrinsic property of ion-velocity should certainly include the quantificational metric of LET and a typical curve of LET versus SEU cross section.

The relevant LET of a heavy ion beam as a function of the ion energy is calculated by SRIM professional version as illustrated in Fig. 6. According to Table 1 and Fig. 2, the corresponding LET values used in this simulation are marked (see the vertical lines in Fig. 6 to characterize the influence of ion energy on the SEU occurrence. It is suggested according to Tables 1 and 2 that LET is a vital factor in inducing the SEU occurrences under the condition of quite different LETs. However, if the corresponding LETs are similar, the peak of LET induced by ion energy should be taken as a basic criterion and then thereby analyze the initial energy density or e^-/h^+ recombination.[8,16]

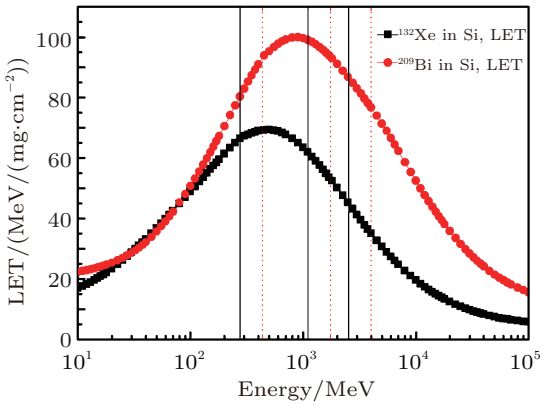


Fig. 6. (color online) Graphical representations of LET values as a function of ion energy for 132Xe and 209Bi in silicon.

Now, we directly evidence the assumption and explanation about there being no obvious difference in magnitude between single errors. The SEU cross section values of the testing device are simultaneously obtained from the experiment and the MUFPSA simulation, which are further fitted by a classic Weibull function, as shown in Fig. 7. The results reveal that the SEU cross-section increases with the increase of LET, and gradually extends to saturation. The Weibull fitting curve indicates that the threshold value of LET inducing the SEU occurrence is about

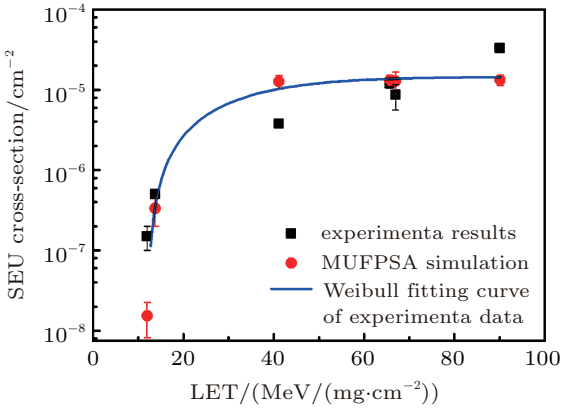


Fig. 7. (color online) Measured and simulated SEU cross sections versus LET of normal incident ions.

12 MeV·cm^2/mg and the saturation of SEU cross section is approximately 1.45×10^{-5} cm^{-2}, which are in good agreement with the results in Table 1. It is reasoned that the LETs of all the incident ions in Table 1 are greater than the threshold LET and then the difference between all resulting SEU cross sections can be taken as being limited.

6. Conclusion

The temporal characteristics from ion-velocity for the SEU occurrences in a specific device are investigated by Monte Carlo simulation. The results display that when the LET of incident ions is greater than the threshold LET, the SEU cross section is slightly influenced by the ion-velocity, which is also confirmed by an experimental result and a simulation result. Meanwhile, the distribution of deposited energies, traversed time, and characterization of the current pulse are shown to depend mainly on the ion-velocity. It is illustrated that the incident ions with larger ion mass values have a larger distribution of deposited energies in the case of the same ion-velocity, the traversed time in the device decreases with the increase of the ion-velocity, and the width variation of the current pulse increases as the ion-velocity decreases. Therefore, as a primary microscopic mechanism of SEU, ion-velocity is non-ignorable for studying in depth the SEU susceptibility to the ionic characteristic.

Acknowledgment

The authors thank the members of the Radiation Harden Center at the Beijing Microelectronics Technology Institute for discussing and supporting the SEU testing experiment.

References

[1] Reed R A, Weller R A, Mendenhall M H, Lauenstein J M, Warren K M, Pellish J A, Schrimpf R D, Sierawski B D, Massengill L W, Dodd P E, Shaneyfelt M R, Felix J A, Schwank J R, Haddad N F, Lawrence R K, Bowman J H and Conde R 2007 *IEEE Trans. Nucl. Sci.* **54** 2312

[2] Dodd P E, Schwank J R, Shaneyfelt M R, Ferlet-Cavrois V, Paillet P, Baggio G, Hash G L, Felix J A, Hirose K and Saito H 2007 *IEEE Trans. Nucl. Sci.* **54** 889

[3] Dodd P E, Schwank J R, Shaneyfelt M R, Felix J A, Paillet P, Ferlet-Cavrois V, Baggio J, Reed R A, Warren K M, Weller R A, Schrimpf R D, Hash G L, Dalton S M, Hirose K and Saito H 2007 *IEEE Trans. Nucl. Sci.* **54** 2303

[4] Constantini J M, Brisard F, Flament J L, Meftah A, Toulemonde M and Hage-Ali M 1992 *Nucl. Instrum. Methods Phys. Res. B* **65** 568

[5] Constantini J M, Rave F, Brisar F, Caput M and Cluzeau C 1993 *Nucl. Instrum. Methods Phys. Res. B* **80/81** 1249

[6] Meftah A, Brisard F, Costantini J M, Hage-Ali M, Stoquert J P, Studer F and Toulemonde M 1993 *Phys. Rev. B* **48** 920

[7] Gaiduk P I, Larsen A N and Hansen J L 2003 *Appl. Phys. Lett.* **83** 1746

[8] Geng C, Liu J, Zhang Z G, Xi K, Gu S, Hou M D, Sun Y M, Duan J L, Yao H J, Mo D and Luo J 2013 *Chin. Phys. C* **37** 066001

[9] Geng C, Liu J, Xi K, Zhang Z G, Gu S and Liu T Q 2013 *Chin. Phys. B* **22** 109501

[10] Waligoriski M P R, Hamm R N and Katz R 1986 *Nucl. Tracks. Radiat. Meas.* **11** 309

[11] Warren K M, Weller R A, Mendenhall M H, Reed R A, Ball D R, Howe C L, Olson B D, Alles M L, Massengill L W, Schrimpf R D, Haddad N F, Doyle S E, McMorrow D, Melinger J S and Lotshaw W T 2005 *IEEE Trans. Nucl. Sci.* **52** 2125

[12] Raine M, Gaillardin M, Sauvestre J, Flament O, Bournel A and Aubry-Fortuna V 2010 *IEEE Trans. Nucl. Sci.* **57** 1892

[13] Raine M, Hubert G, Gaillardin M, Paillet P and Bournel A 2011 *IEEE Trans. Nucl. Sci.* **58** 2607

[14] Raine M, Gaillardin M, Paillet P, Duhamel O, Girard S and Bournel A 2011 *IEEE Trans. Nucl. Sci.* **58** 2664

[15] Geng C, Liu J, Xi K, Zhang Z G, Gu S and Liu T Q 2012 *IMP & HIRFL Annual Report* p. 120

[16] Geng C, Liu J, Xi K, Zhang Z G, Gu S, Hou M D, Sun Y M, Duan J L, Yao H J and Mo D 2013 *Chin. Phys. B* **22** 059501